UCLA
UCLA Previously Published Works

Title

Mechanism and Origins of Chemo- and Stereoselectivities of Aryl Iodide-Catalyzed Asymmetric Difluorinations of β-Substituted Styrenes

Permalink

https://escholarship.org/uc/item/8d80t91m

Journal

Journal of the American Chemical Society, 140(45)

ISSN

0002-7863

Authors

Zhou, Biying
Haj, Moriana K
Jacobsen, Eric N
et al.

Publication Date

2018-11-14

DOI

10.1021/jacs.8b05935

Peer reviewed

eScholarship.org Powered by the California Digital Library
University of California

Author Manuscript

Author Manuscript

Author Manuscript

Author Manuscript

HHS Public Access

Author manuscript

J Am Chem Soc. Author manuscript; available in PMC 2019 November 14.

Published in final edited form as:

J Am Chem Soc. 2018 November 14; 140(45): 15206–15218. doi:10.1021/jacs.8b05935.

Mechanism and Origins of Chemo- and Stereoselectivities of Aryl Iodide-Catalyzed Asymmetric Difluorinations of β-Substituted Styrenes

Biying Zhou[†], **Moriana K. Haj**[±], **Eric N. Jacobsen**[±], **K. N. Houk**[‡], and **Xiao-Song Xue**[†,‡]

[†] State Key Laboratory of Elemento-Organic Chemistry, College of Chemistry, Nankai University, Tianjin 300071, China

[‡] Department of Chemistry and Biochemistry, University of California, Los Angeles, California 90095, United States

[±] Department of Chemistry and Chemical Biology, Harvard University, Cambridge, Massachusetts 02138, United States

Abstract

The mechanism of the aryl iodide-catalyzed asymmetric migratory geminal difluorination of *β*-substituted styrenes (Banik et al. *Science* **2016**, 353, 51) has been explored with density functional theory computations. The computed mechanism consists of (a) activation of iodoarene difluoride (**ArIF$_2$**), (b) enantiodetermining 1, 2-fluoroiodination, (c) bridging phenonium ion formation via S_N2 reductive displacement, and (d) regioselective fluoride addition. According to the computational model, the **ArIF$_2$** intermediate is stabilized through halogen-**π** interactions between the electron-deficient iodine(III) center and the benzylic substituents at the catalyst stereogenic centers. Interactions with the catalyst ester carbonyl groups (I(III)$^+$···O) are not observed in the unactivated complex, but do occur upon activation of **ArIF$_2$** through hydrogen bonding interactions with external Brønsted acid (HF). The 1, 2-fluoroiodination occurs via alkene complexation to the electrophilic, cationic I(III) center followed by C−F bond formation anti to the forming C−I bond. The bound olefin and the C−I bond of catalyst adopt a spiro-arrangement in the favored transition structures but a nearly periplanar arrangement in the disfavored transition structures. Multiple attractive non-covalent interactions, including slipped **π**···**π** stacking, C–H···O, and C–H···**π** interactions, are found to underlie the high asymmetric induction. The chemoselectivity for 1,1-difluorination versus 1,2-difluorination is controlled mainly by 1) the steric effect of the substituent on the olefinic double bond, and 2) the nucleophilicity of the carbonyl oxygen of substrate.

Graphical Abstract

Corresponding Author xuexs@nankai.edu.cn, houk@chem.ucla.edu.

The authors declare no competing financial interest.

DEDICATION

We dedicate this work to Professor Jin-Pei Cheng on the occasion of his 70th birthday.

ASSOCIATED CONTENT

Supporting Information.

Figure S1-S13, and optimized geometries of all species. This material is available free of charge via the Internet at http://pubs.acs.org.

Author Manuscript Author Manuscript Author Manuscript Author Manuscript

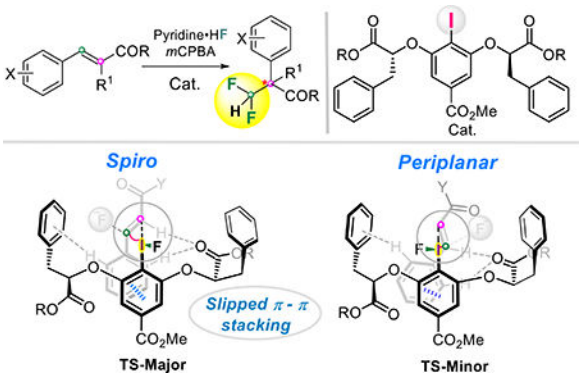

INTRODUCTION

Hypervalent iodine compounds have in recent years evolved from chemical curiosities into mainstream reagents in organic synthesis.[1] They possess reactivities similar to those of transition metals, but potentially practical advantages with respect to toxicity and cost. The discovery of enantioselective molecular catalysts based on iodine (I/III) redox chemistry has added a new dimension to hypervalent iodine chemistry.[2] Many chiral hypervalent iodine reagents or catalysts (Figure 1) have been invented by the groups of Wirth,[3] Kita,[4] Ishihara,[5] Fujita,[6] Muñiz,[7] Legault[8], and others,[9] to effect asymmetric transformations that would be difficult to accomplish otherwise.[2,10]

One of our groups in 2016 reported a catalytic, asymmetric, migratory geminal difluorination of *β*-substituted styrenes to access a variety of products bearing difluoromethylated tertiary or quaternary stereocenters (Scheme 1a).[11] The difluoromethyl group (CHF_2) has received special attention[12] because it serves as a bioisostere of hydroxyl and thiol groups[13], and also as a lipophilic hydrogen bond donor.[14] The simple C_2-symmetric aryl iodide catalyst plus *m*-chloroperbenzoic acid and hydrogen fluoride can generate chiral difluoromethyl groups from reaction with the double bond of styrene derivatives. The catalyst bearing benzyl substituents **(ArI-1)** induces higher enantioselectivity than its 3,4,5-trifluorophenyl (**ArI-2**) and aliphatic (**ArI-3**) analogs (Scheme 1b). It was hypothesized that cationic intermediates and/or transition structures are stabilized selectively through attractive cation-**π** interactions. A chemoselectivity switch was observed based on subtle changes in substrate structure, with the 1,1-difluorination product formed by difluorination of disubstituted cinnamamides or trisubstituted cinnamate ester derivatives (Scheme 1a-b), but the 1,2-difluorination product obtained in the difluorination of the trisubstituted cinnamamide derivative **S3** (Scheme 1c). We report here a computational study of the mechanism and origins of chemo- and stereoselectivities in these systems, and advance a model of how these hypervalent catalysts achieve such remarkable selectivity.

COMPUTATIONAL METHODS

Quantum chemical calculations were performed using the Gaussian 09 suite of programs.[15] Geometry optimizations and frequencies were calculated with the M06–2X[16] density

Author Manuscript Author Manuscript Author Manuscript Author Manuscript

functional and a mixed basis set of LANL2DZ[17] for I and 6–31G(d, p) for other atoms in conjunction with the SMD[18] implicit solvation model to account for the solvation effects of dichloromethane. Optimized geometries were verified by frequency computations as minima (zero imaginary frequencies) or transition structures (a single imaginary frequency) at the same level of theory. More accurate electronic energies were obtained by single point energy calculations at the SMD-M06–2X/6–311++G(d, p)+SDD(I)[19] level of theory.[20] A number of previous computational studies of hypervalent iodine-mediated reactions have employed the M06–2X functional.[21]

Because of the flexibility of the hypervalent iodoarene catalyst,[20b,22] a conformational study was performed on the active catalyst iodoarene difluoride, intermediates, and transition structures. The lowest energy conformers are discussed in the following sections, while other higher energy conformers are given in the Supporting Information. A factor of $RT\ln(24.46)$ was added to free energy for each species to account for the 1 atm to 1 M standard state change. All Gibbs energies in solution reported throughout the text are in kcal mol^{-1}, and the bond lengths are in Å ngstroms (Å). NCIPLOT[23] and Multiwfn[24] were employed for the visualization of noncovalent interactions and topology analysis, respectively. The structures were generated by CYLview[25] and VMD[26].

RESULTS AND DISCUSSION

Model Reaction and Proposed Catalytic Cycle.

In the original experimental studies, it was shown that the benzylic substituents at the catalyst stereogenic centers are essential for high enantioselectivity, while the alkyl ester groups on the stereocenter-bearing arms do not have a significant influence on enantioselectivity.[11,27] We first explored the difluorination of cinnamamide S1 catalyzed by aryl iodide **ArI-4** (Scheme 2a). Subsequently, the stereocontrolling TSs for **ArI-1–ArI-3**-catalyzed geminal difluorination of cinnamate ester S2 (Scheme 2b) were studied to investigate effects of catalyst modification on enantioselectivities. Finally, **ArI-4** catalyzed enantioselective 1,2-difluorination of cinnamamide **S3** (Scheme 2c) was studied to determine the origin of chemoselectivity.

The mechanism proposed in the initial study for aryl iodide-catalyzed asymmetric migratory geminal difluorination is shown in Scheme 3.[11] Oxidation and deoxyfluorination of aryl iodide precursor **ArI-4** gives the iodoarene difluoride **$ArIF_2$-4**. **$ArIF_2$-4** is further activated by HF, and undergoes an enantioselective 1,2-fluoroiodination of **S1** to provide **3+**, followed by the stereospecific formation of phenonium ion **4** and regeneration of **ArI-4**. The final regioselective fluoride attack on **4** affords the 1, 1-difluorination product. The computed reaction coordinate diagram shown in Figure 3 starts from **$ArIF_2$-4** described in Figure 2.[11,28] The relative energies are SMD-M06–2X/6–311++G(d,p)-SDD(I)//SMD-M06–2X/6–31G(d,p)-LANL2DZ(I) computed Gibbs free energies, unless specifically noted.

Conformations of the Active Hypervalent Iodoarene Catalyst, $ArIF_2$-4.

We first explored the conformation of the active catalyst **$ArIF_2$-4**. Previous single crystal X-ray structural analysis[5c,7c,22b] as well as Sunoj and co-worker's computational studies[22a] on

Author Manuscript Author Manuscript Author Manuscript Author Manuscript

(diacetoxyiodo)arene bearing lactic esters and amides have demonstrated the C_2-symmetric helical chirality around the central iodine atom. The conformational space of the active catalyst **ArIF$_2$-4** was studied here. Figure 2 shows the lowest energy conformer of **ArIF$_2$-4** (other high-energy conformers are presented in Figure S1). A helical C_2-symmetric chirality around the central iodine atom is observed. The benzylic group at the stereogenic center was found to have a unique effect on conformation. In **ArIF$_2$-4**, the center of the aromatic ring of the benzylic group points toward to the iodine(III) center, indicating the presence of attractive halogen bonding interactions[29] between the electron-deficient iodine(III) center and the electron-rich aromatic rings.[30] Other conformers without the halogen-π interactions are at least 1.7 kcal mol^{-1} less stable (Figure S1).

Mechanism of Aryl Iodide-Catalyzed Migratory Geminal Difluorination of Cinnamamide.

The computed potential energy profile for **ArIF$_2$-4** catalyzed asymmetric migratory geminal difluorination of cinnamamide S1 is summarized in Figure 3. Optimized geometries of some key transition structures and intermediates are presented in Figure 4. The first step is the activation of the iodoarene difluoride **ArIF$_2$-4** by HF to generate the active catalytic species **1a+**.[4c,28b,28c,31] The formation of the hydrogen-bonded complex **1-HF** is endergonic by 1.5 kcal mol^{-1}.[32] The free energy of activation for the transformation of **ArIF$_2$-4** to **1a+** via **TS1a-HF** is 19.0 kcal mol^{-1}. Although a single HF activation model for iodoarene difluorides has been proposed,[4c,28b,31a,31e] multiple HF molecules (or even pyridine•H$^+$) likely participate because a large excess of pyridine•9HF is employed in these reactions. The activation barrier to ionization of **ArIF$_2$-4** is reduced to 13.7 kcal mol^{-1} (**TS1a-2HF**) when two molecules of HF engage in activation, and no further reduction in barrier was predicted computationally when three molecules of HF (or pyridine•H$^+$) participate in activation (**TS1a-3HF:** $\Delta G^{\ddagger}$= 15.3 kcal mol^{-1}; **TS1a-PyrH$^+$**: $\Delta G^{\ddagger}$= 18.2 kcal mol^{-1}; **TS1a-HF-PyrH$^+$**: $\Delta G^{\ddagger}$= 17.2 kcal mol^{-1}, See Figure S2). The transformation of **ArIF$_2$-4** to **1a+** is also assisted by the ester carbonyl group on the side chain through an I(III)$^+$···O interaction that stabilizes the incipient cationic iodonium (Figure 3).[33]An I(III)$^+$···O interaction was proposed and confirmed by X-ray structural analysis by Wirth and co-workers.[3a,3b,34] More recently, Fujita and co-workers also reported that such a I(III)$^+$···O interaction exists even in acetonitrile.[6b] The formation of the strong I(III)$^+$···O interaction in **1a+** induces a conformational change of the benzylic group, resulting in disruption of halogen-π interactions and exposure of the highly electrophilic cationic I(III) center for subsequent substrate binding and activation.

In the following step, **1a+** coordinates to the *Si*-face of the olefin substrate S1 through an I(III)$^+$···π interaction, leading to a catalyst-substrate adduct **2**, which lies 1.4 kcal mol^{-1} below **1a+** (Figure 3). The nucleophilic attack of fluoride on the exposed *Re*-face of the olefin of adduct **2** (Figure 5) leads to intermediate **3** with a barrier of 6.7 kcal mol^{-1} (via **TS2a-S**) with respect to **2**. The *syn* 1,2- fluoroiodination (***syn*-TS2a-S**) is 10.8 kcal mol^{-1} less favorable than the *anti* 1,2-fluoroiodination (**TS2a-S**). Additionally, the barrier for nucleophilic attack of pyridine•HF (Olah's reagent)[35] to the alkene complex **2** is 9.6 kcal mol^{-1} (**TS2a-S-pyrHF**), which is 2.9 kcal mol^{-1} higher than that for nucleophilic attack of $^-F(HF)_2$. The formation of the C−I bond significantly weakens the I−F bond in intermediate **3** (I−F bond length 1.91 Å in **2** versus 2.09 Å in **3**: Figure 4). Consequently, the I−F bond in

Author Manuscript Author Manuscript Author Manuscript Author Manuscript

intermediate **3** is prone to dissociation under the activation of HF to provide a more stable intermediate **3+**, which is also stabilized by an $I(III)^{+}\cdots O$ interaction and is exergonic by 20.7 kcal mol^{-1} from **3**.

The aryliodonium moiety in **3+** is an excellent leaving group. It is displaced intramolecularly by nucleophilic attack of the phenyl ring in the cinnamamide, leading to the stereospecific formation of phenonium ion **4** and regeneration of **ArI-4**. The calculated barrier of the reductive displacement via an S_N2-like transition state **TS3a** is 18.9 kcal mol^{-1} relative to **3+** (Figure 3). The last step of the reaction mechanism is the regioselective fluoride addition to afford the chiral geminal difluorination product. The computations predict that the fluoride $F^{-}(HF)_2$ addition to the F-substituted carbon atom through **TS4** is facile, with a barrier of only 0.3 kcal mol^{-1} relative to **4**. Addition to the $CONH_2$-bearing carbon atom (**TS4–2**) is 10.7 kcal mol^{-1} less favorable, which is in line with our previous findings.[36] The formation of **P1** is highly exergonic by 63.1 kcal mol^{-1}.

Reviewing the computed energy profile of the overall reaction pathway,[37] the 1,2-fluoroiodination is the stereocontrolling step. This step generates the C*−F and C*−I stereocenters. The chirality of the former is preserved in the subsequent reductive displacement and fluoride addition.

Origin of Enantioselectivity.

The lowest-energy TSs leading to the major and minor enantiomers are shown in Figure 5. In **TS2a-S,** the *Si*-face of the olefinic double bond of cinnamamide coordinates to the $I(III)^{+}$ center of catalyst, while the incoming fluoride attacks the exposed *Re*-face, giving rise to the experimentally observed major (*S*)-product after reductive displacement and fluoride addition. In **TS2a-R**, the *Re*-face of olefinic double bond coordinates to the $I(III)^{+}$ center, and nucleophilic attack of fluoride takes place at the *Si*-face. The computed activation energy difference between **TS2a-S** and **TS2a-R** is 2.2 kcal mol^{-1}.[38] This corresponds to an enantiomeric excess of 95% in favor of the *S* enantiomer, which agrees qualitatively with the level and sense of enantioselectivity observed experimentally (86% *S ee*). Jacobsen and co-workers have demonstrated experimentally that the benzylic substituents at the catalyst stereogenic centers are essential for high enantioselectivity in the geminal difluorination reaction, while the ester alkyl group on the chiral arms does not have a significant influence on enantioselectivity.[11,27] Examination of the computed transition state structures leading to the major and minor enantiomers provides some insight into potential structural reasons for this observation.

As depicted in Figure 5, the phenyl group of cinnamamide adopts a similar binding arrangement in both transition structures. This causes the double bond to be oriented differently in the two TSs. The olefin (C12−C13) of cinnamamide and the C1−I2 bond of catalyst is in spiro-arrangement in **TS2a-S**, but it is nearly periplanar in **TS2a-R** (the dihedral angle θ1 between the Cl−I2 and C12−C13 bonds is 81.5° in **TS2a-S** vs −16.4° in **TS2a-R**, Figure 5). We define a spiro-arrangement as θ1 = 90 ± 30° and periplanar as θ1 = 0 ± 30° Thus, **TS2a-R** is destabilized by torsional strain.[39] We calculated the corresponding TSs (**TS2a-S-M** and **TS2a-R-M)** with the catalyst stereogenic centers being replaced by

Author Manuscript Author Manuscript Author Manuscript Author Manuscript

methyl groups (Figure 6a). **TS2a-S-M** and **TS2a-R-M** are enantiomeric, wherein the double bond and the C1−I2 bond is in spiro-arrangement with identical dihedral angle θ1 (θ1 = 79.2° in **TS2a-S-M** vs –79.2° in **TS2a-R-M**). Comparing energy differences between **TS2a-R-M** and **TS2a-R-M-distorted** indicates that the spiro-arrangement is more favorable than the periplanar-arrangement by roughly 6.6 kcal mol^{-1} (Figure 6a).

A closer inspection of the two transition structures (Figure 5) reveals that there is a stabilizing π···π stacking interaction[40,41] between the phenyl of cinnamamide and the electron-deficient iodoaryl ring of the catalyst[42] (optimized TSs without π···π stacking were at least 7 kcal mol^{-1} less stable see Figure S5). The π···π stacking interaction provides a driving force for the phenyl group of substrate to be deeply buried in the catalyst's chiral pocket (Figure 6b). When the *Si*-face of the olefinic double bond coordinates to the $I(III)^+$ center, the phenyl is well accommodated in a binding pocket, and the double bond and the C1−I2 bond can adopt an ideal spiro-arrangement (**TS2a-S** and **TS2a-S-M** have nearly identical dihedral θ1). However, when the *Re*face of substrate **S1** coordinates in a similar manner to the $I(III)^+$ center of catalyst, the phenyl group of cinnamamide will clash with the ester carbonyl group at the stereocenter-bearing arm of catalyst. Consequently, the chiral catalyst forces **TS2a-R** to be distorted away from the ideal spiro structure in order to accommodate the cinnamamide phenyl into the stabilizing pocket (Figure 6b). These results suggest that the π···π stacking interaction plays a crucial role in stereoinduction in this reaction. This model also accounts for the experimental observation that the reaction conducted with (Z)-methyl cinnamate proceeds with low enantioselectivity (Figure 7). This is mainly because of loss of stabilizing π···π stacking interactions due to improper spatial arrangement.[43]

It should be noted that other favorable noncovalent interactions[44], including C–H···O[45] and C−H···π interactions[40a,46], are also developed between the substrate and the catalyst's chiral pocket. However, these stabilizing interactions do not appear to contribute singificantly to enantiocontrol, as their strengths were estimated to be of approximately the same order of magnitude in **TS2a-S** and **TS2a-R**[41c,47,48] (Figure S9).

Impact of Catalyst Modification on Enantioselectivity.

To understand the influence of catalyst modifications on enantioselectivity, the stereocontrolling TSs for **ArI-1–ArI-3**-promoted geminal difluorination of cinnamate ester **S2** were studied. The calculated transition structures together with their relative free energies and *ee* values are given in Figure 8. The calculated *ee* values are 99% ($\Delta\Delta G^{\ddagger}$:3.0 kcal mol^{-1}) for **ArI-1**, −84% ($\Delta\Delta G^{\ddagger}$: −1.2 kcal mol^{-1}) for **ArI-2**, and −68% ($\Delta\Delta G^{\ddagger}$: −0.8 kcal mol^{-1}) for **ArI-3**, which are in reasonable agreement with the experimentally observed trend in these values: 94% for **ArI-1**, −77% for **ArI-2** and −60% for **ArI-3**.[11]

The olefinic double bond of the cinnamate ester and the C1−I2 bond of catalyst adopt a nearly spiro-arrangement in all three favored TS structures but a periplanar-arrangement in disfavored TS structures (Figure 8). Replacing the phenyl with the more electron-deficient 3,4,5-trifluorophenyl (a weaker π-donator) results in a longer C−H···π distance in **TS2c-R** (2.46 Å in **TS2b-S vs** 2.49 Å in **TS2c-R**). Thus, the C−H···π interaction would contribute a

Author Manuscript Author Manuscript Author Manuscript Author Manuscript

lesser extent to the stabilization of the favored **TS2c-R**. Additionally, a more acidic C−H bond in 3,4,5-trifluorophenyl than in phenyl enables formation of a C−H···O interaction with the ester carbonyl group of substrate in **TS2c-S** with C−H···O distance of 2.67 Å. Thus, the observed lower selectivity of **ArI-2** can be mainly attributed to two factors: 1) attenuation of the C−H···π interaction in the TS leading the major stereoisomer, and 2) strengthening of the C−H···O interaction in the TS leading the minor stereoisomer. Replacement of the phenyl with cyclohexyl results in disruption of C−H···π interactions and repulsion between the phenyl ring of the cinnamate ester and the cyclohexyl of catalyst (Figure 8). These results are consistent with the experimental observation that incorporation of poorly π-donating substituents on the catalyst stereogenic center has a pronounced deleterious effect on enantioselectivity.[22a]

Origin of Chemoselectivity.

We also explored the origin of altered chemoselectivity in the α-isopropyl cinnamamide (Scheme 4). It was proposed that 1,1-difluorination proceeds via skeletal rearrangement with the phenyl as a nucleophile, while 1,2-difluorination occurs when the carbonyl of the cinnamamide acts as the nucleophilic group (Scheme 4).[11] We have calculated the transition state structures that determine the chemoselectivity of aryl iodide-catalyzed enantioselective difluorination of substrates **S1**, **S2**, and **S3**. The results are presented in Figure 9. For **S1** and **S2**, nucleophilic attack by the phenyl group (**TS3a-S1** and **TS3a-S2)** was found to 3.5 kcal mol^{-1} and 6.4 kcal mol^{-1} more favorable than by the carbonyl group (**TS3a'-S1** and **TS3a'-S2**), respectively. This is consistent with the experimental observation that reactions of **S1** and **S2** afford 1, 1-difluorination product with complete chemoselectivity. A greater energy difference between **TS3a-S2** and **TS3a'-S2** ($\Delta\Delta G^{\ddagger}$: 6.4 *vs.* 3.5 kcal mol^{-1}) can be attributed to a lower nucleophilicity of the carbonyl group in **S2** as indicated by the calculated NPA charges (Figure 9).

For α-isopropyl cinnamamide S3, nucleophilic attack by the phenyl group **TS3a-S3** becomes 3.5 kcal mol^{-1} less favorable than by the carbonyl group **TS3a'-S3**, consistent with the experimental observation that only 1, 2-difluorination product is detected.[11] A closer look into the structure of **TS3a-S3** reveals that nucleophilic attack of C12 by the phenyl group suffers from steric repulsion between the phenyl and ^{i}Pr groups. The steric effect of the ^{i}Pr group is largely attenuated when the small carbonyl oxygen of the amide acts as nucleophile.

CONCLUSION

We have developed a computational model to account for the chemoselectivity and stereoselectivity of aryl iodidecatalyzed asymmetric difluorinations of β-substituted styrenes. In the transition structures leading to the major enantiomers, the styrenyl olefin and the C−I bond of catalyst adopt a spiro-arrangement, and the phenyl group of the substrate is accommodated in a binding pocket. Although the minor TS has similar binding of the phenyl, this forces a less favorable nearly periplanar-arrangement in the transition structures leading to the minor enantiomers. A slipped π···π stacking interaction between the phenyl group of substrate and the electron-deficient iodoaryl ring of catalyst plays a crucial role in

Author Manuscript Author Manuscript Author Manuscript Author Manuscript

stereoinduction of these reactions. The model proposed here may serve as a useful starting point for future analyses of enantioselective alkene difunctionalization reactions catalyzed by C_2-symmetric chiral aryl iodides.

Supplementary Material

Refer to Web version on PubMed Central for supplementary material.

ACKNOWLEDGMENT

We are grateful for the financial support from the Natural Science Foundation of China (Grant 21772098 to X.X.S.), the NSF (CHE-1361104 to K.N.H.), the NIH (GM-43214 to E.N.J.), Nankai-UCLA Excellent Young Researcher program, and the Fundamental Research Funds for the Central Universities. X.S.X appreciates the hospitality provided by Professor K. N. Houk (UCLA).

REFERENCES

(1). (a)Zhdankin VV; Stang PJ, Chemistry of Polyvalent Iodine. Chem. Rev 2008, 108, 5299 [PubMed: 18986207] (b)Zhdankin VV, Hypervalent Iodine Chemistry: Preparation, Structure, and Synthetic Applications of Polyvalent Iodine Compounds; Wiley: 2013(c)Zhdankin VV Hypervalent Iodine Chemistry; John Wiley & Sons: Chichester, 2014(d)Yoshimura A; Zhdankin VV, Advances in Synthetic Applications of Hypervalent Iodine Compounds Chem. Rev 2016, 116, 3328 [PubMed: 26861673] (e)Hypervalent Iodine Chemistry; Wirth T, Ed.; Springer-Verlag: Berlin, 2016.

(2). Selected review on chiral hypervalent iodine catalysts: Richardson RD; Wirth T, Hypervalent Iodine Goes Catalytic. Angew. Chem. Int. Ed 2006, 45, 4402Dohi T; Kita Y, Hypervalent Iodine Reagents as a New Entrance to Organocatalysts. Chem. Commun 2009, 2073Liang H; Ciufolini MA, Chiral Hypervalent Iodine Reagents in Asymmetric Reactions. Angew. Chem. Int. Ed 2011, 50, 11849Uyanik M; Ishihara K, Catalysis with In Situ-Generated (Hypo)iodite Ions for Oxidative Coupling Reactions. ChemCatChem 2012, 4, 177Parra A; Reboredo S, Chiral Hypervalent Iodine Reagents: Synthesis and Reactivity. Chem. Eur. J 2013, 19, 17244 [PubMed: 24272963] Romero RM; Wöste TH; Muñiz K, Vicinal Difunctionalization of Alkenes with Iodine (III) Reagents and Catalysts. Chem. Asian J 2014, 9, 972 [PubMed: 24591421] Singh FV; Wirth T, Hypervalent Iodine-Catalyzed Oxidative Functionalizations Including Stereoselective Reactions. Chem. Asian J 2014, 9, 950 [PubMed: 24523252] Berthiol F, Reagent and Catalyst Design for Asymmetric Hypervalent Iodine Oxidations. Synthesis 2015, 47, 587Lauriers AJD; Legault CY, Enol and Ynol Surrogates: Promising Substrates for Hypervalent Iodine Chemistry. Asian J. Org. Chem 2016, 5, 1078Basdevant B; Guilbault A-A; Beaulieu S; Jobin-Des Lauriers A; Legault CY, Iodine (III)-Mediated Synthesis of Chiral α-Substituted Ketones: Recent Advances and Mechanistic Insights. Pure Appl. Chem 2017, 89, 781Claraz A; Masson G, Asymmetric Iodine Catalysis-Mediated Enantioselective Oxidative Transformations. Org. Biomol. Chem 2018, 16, 5386 [PubMed: 30024581] Li X; Chen P; Liu G, Recent Advances in Hypervalent Iodine(III)-Catalyzed Functionalization of Alkenes. Beilstein J. Org. Chem 2018, 14, 1813. [PubMed: 30112085]

(3). (a)Hirt UH; Spingler B; Wirth T, New Chiral Hypervalent Iodine Compounds in Asymmetric Synthesis. J. Org. Chem 1998, 63, 7674(b)Hirt Urs H.; Schuster Martin F. H.; French Andrew N.; Wiest Olaf G.; Wirth T, Chiral Hypervalent Organo-Iodine(III) Compounds. Eur. J. Org. Chem 2001, 2001, 1569(c)Richardson RD; Page TK; Altermann S; Paradine SM; French AN; Wirth T, Enantioselective α-Oxytosylation of Ketones Catalysed by Iodoarenes. Synlett 2007, 2007, 0538(d)Altermann SM; Richardson RD; Page TK; Schmidt RK; Holland E; Mohammed U; Paradine SM; French AN; Richter C; Bahar AM; Witulski B; Wirth T, Catalytic Enantioselective α-Oxysulfonylation of Ketones Mediated by Iodoarenes. Eur. J. Org. Chem 2008, 2008, 5315(e)Farid U; Wirth T, Highly Stereoselective Metal-Free Oxyaminations Using Chiral Hypervalent Iodine Reagents. Angew. Chem. Int. Ed 2012, 51, 3462(f)Farid U; Malmedy F; Claveau R; Albers L; Wirth T, Stereoselective Rearrangements with Chiral Hypervalent Iodine Reagents. Angew. Chem. Int. Ed 2013, 52, 7018(g)Mizar P; Laverny A; El-Sherbini M; Farid U;

Author Manuscript Author Manuscript Author Manuscript Author Manuscript

Brown M; Malmedy F; Wirth T, Enantioselective Diamination with Novel Chiral Hypervalent Iodine Catalysts. Chem. Eur. J 2014, 20, 9910 [PubMed: 25042733] (h)Mizar P; Niebuhr R; Hutchings M; Farooq U; Wirth T, Thioamination of Alkenes with Hypervalent Iodine Reagents. Chem. Eur. J 2016, 22, 1614 [PubMed: 26660291] (i)Brown M; Kumar R; Rehbein J; Wirth T, Enantioselective Oxidative Rearrangements with Chiral Hypervalent Iodine Reagents. Chem. Eur. J 2016, 22, 4030 [PubMed: 26800241] (j)Qurban J; Elsherbini M; Wirth T, Electron-Deficient Chiral Lactic Acid-Based Hypervalent Iodine Reagents. J. Org. Chem 2017, 82, 11872. [PubMed: 28727455]

(4). (a)Dohi T; Maruyama A; Takenaga N; Senami K; Minamitsuji Y; Fujioka H; Caemmerer SB; Kita Y, A Chiral Hypervalent Iodine(III) Reagent for Enantioselective Dearomatization of Phenols. Angew. Chem. Int. Ed 2008, 47, 3787(b)Dohi T; Takenaga N; Nakae T; Toyoda Y; Yamasaki M; Shiro M; Fujioka H; Maruyama A; Kita Y, Asymmetric Dearomatizing Spirolactonization of Naphthols Catalyzed by Spirobiindane-Based Chiral Hypervalent Iodine Species. J. Am. Chem. Soc 2013, 135, 4558 [PubMed: 23445490] (c)Suzuki S; Kamo T; Fukushi K; Hiramatsu T; Tokunaga E; Dohi T; Kita Y; Shibata N, Iodoarene-Catalyzed Fluorination and Aminofluorination by an Ar-I/HF·Pyridine/mCPBA System. Chem. Sci 2014, 5, 2754(d)Ogasawara M; Sasa H; Hu H; Amano Y; Nakajima H; Takenaga N; Nakajima K; Kita Y; Takahashi T; Dohi T, Atropisomeric Chiral Diiododienes (Z,Z)-2,3-Di(1-iodoalkylidene)tetralins: Synthesis, Enantiomeric Resolution, and Application in Asymmetric Catalysis. Org. Lett 2017, 19, 4102 [PubMed: 28726416] (e)Dohi T; Sasa H; Miyazaki K; Fujitake M; Takenaga N; Kita Y, Chiral Atropisomeric 8,8'-Diiodobinaphthalene for Asymmetric Dearomatizing Spirolactonizations in Hypervalent Iodine Oxidations. J. Org. Chem 2017, 82, 11954. [PubMed: 28982239]

(5). (a)Uyanik M; Okamoto H; Yasui T; Ishihara K, Quaternary Ammonium (Hypo)iodite Catalysis for Enantioselective Oxidative Cycloetherification. Science 2010, 328, 1376 [PubMed: 20538945] (b)Uyanik M; Yasui T; Ishihara K, Enantioselective Kita Oxidative Spirolactonization Catalyzed by In Situ Generated Chiral Hypervalent Iodine(III) Species. Angew. Chem. Int. Ed 2010, 49, 2175(c)Uyanik M; Yasui T; Ishihara K, Hydrogen Bonding and Alcohol Effects in Asymmetric Hypervalent Iodine Catalysis: Enantioselective Oxidative Dearomatization of Phenols. Angew. Chem. Int. Ed 2013, 52, 9215(d)Uyanik M; Yasui T; Ishihara K, Chiral Hypervalent Organoiodine-Catalyzed Enantioselective Oxidative Spirolactonization of Naphthol Derivatives. J. Org. Chem 2017, 82, 11946 [PubMed: 28926246] (e)Uyanik M; Sasakura N; Mizuno M; Ishihara K, Enantioselective Synthesis of Masked Benzoquinones Using Designer Chiral Hypervalent Organoiodine(III) Catalysis. ACS Catal. 2017, 7, 872.

(6). (a)Fujita M; Okuno S; Lee HJ; Sugimura T; Okuyama T, Enantiodifferentiating Tetrahydrofuranylation of But-3-Enyl Carboxylates Using Optically Active Hypervalent Iodine(III) Reagents via a 1,3-Dioxan-2-yl Cation Intermediate. Tetrahedron Lett. 2007, 48, 8691(b)Fujita M; Yoshida Y; Miyata K; Wakisaka A; Sugimura T, Enantiodifferentiating endo-Selective Oxylactonization of *ortho*-Alk-1-enylbenzoate with a Lactate-Derived Aryl-λ^3-Iodane. Angew. Chem. Int. Ed 2010, 49, 7068(c)Fujita M; Wakita M; Sugimura T, Enantioselective Prevost and Woodward Reactions Using Chiral Hypervalent Iodine(III): Switchover of Stereochemical Course of an Optically Active 1,3-Dioxolan-2-yl Cation. Chem. Commun 2011, 47, 3983(d)Fujita M; Mori K; Shimogaki M; Sugimura T, Asymmetric Synthesis of 4,8-Dihydroxyisochroman-1-one Polyketide Metabolites Using Chiral Hypervalent Iodine(III). Org. Lett 2012, 14, 1294 [PubMed: 22335341] (e)Takesue T; Fujita M; Sugimura T; Akutsu H, A Series of Two Oxidation Reactions of ortho-Alkenylbenzamide with Hypervalent Iodine(III): A Concise Entry into (3R,4R)-4-Hydroxymellein and (3R,4R)-4-Hydroxy-6-methoxymellein. Org. Lett 2014, 16, 4634 [PubMed: 25158282] (f)Shimogaki M; Fujita M; Sugimura T, Metal-Free Enantioselective Oxidative Arylation of Alkenes: Hypervalent-Iodine-Promoted Oxidative C−C Bond Formation. Angew. Chem. Int. Ed 2016, 55, 15797(g)Shimogaki M; Fujita M; Sugimura T, Enantioselective C–C Bond Formation during the Oxidation of 5-Phenylpent-2-enyl Carboxylates with Hypervalent Iodine(III). J. Org. Chem 2017, 82, 11836. [PubMed: 28551992]

(7). (a)Röben C; Souto JA; González Y; Lishchynskyi A; Muñiz K, Enantioselective Metal-Free Diamination of Styrenes. Angew. Chem. Int. Ed 2011, 50, 9478(b)Romero RM; Souto JA; Muñiz K, Substitution Effects of Hypervalent Iodine(III) Reagents in the Diamination of Styrene. J. Org. Chem 2016, 81, 6118 [PubMed: 27310710] (c)Haubenreisser S; Wöste TH; Martínez C; Ishihara K; Muñiz K, Structurally Defined Molecular Hypervalent Iodine Catalysts for Intermolecular

Author Manuscript Author Manuscript Author Manuscript Author Manuscript

Enantioselective Reactions. Angew. Chem. Int. Ed 2016, 55, 413(d)Muñiz K; Barreiro L; Romero RM; Martínez C, Catalytic Asymmetric Diamination of Styrenes. J. Am. Chem. Soc 2017, 139, 4354. [PubMed: 28277652]

(8). (a)Guilbault A-A; Basdevant B; Wanie V; Legault CY, Catalytic Enantioselective α-Tosyloxylation of Ketones Using Iodoaryloxazoline Catalysts: Insights on the Stereoinduction Process. J. Org. Chem 2012, 77, 11283 [PubMed: 23234479] (b)Basdevant B; Legault CY, Enantioselective Iodine(III)-Mediated Synthesis of α-Tosyloxy Ketones: Breaking the Selectivity Barrier. Org. Lett 2015, 17, 4918 [PubMed: 26378799] (c)Jobin-Des Lauriers A; Legault CY, Iodine(III)-Mediated Oxidative Hydrolysis of Haloalkenes: Access to α-Halo Ketones by a Release-and-Catch Mechanism. Org. Lett 2016, 18, 108. [PubMed: 26679382]

(9). (a)Ray DG; Koser GF, Iodinanes with Iodine(III)-Bound Homochiral Alkoxy Ligands: Preparation and Utility for the Synthesis of Alkoxysulfonium Salts and Chiral Sulfoxides. J. Am. Chem. Soc 1990, 112, 5672(b)Ochiai M; Kitagawa Y; Takayama N; Takaoka Y; Shiro M, Synthesis of Chiral Diaryliodonium Salts, 1,1'-Binaphthyl-2-yl(phenyl)iodonium Tetrafluoroborates: Asymmetric α-Phenylation of β-Keto Ester Enolates. J. Am. Chem. Soc 1999, 121, 9233;(c)Boppisetti JK; Birman VB, Asymmetric Oxidation of o-Alkylphenols with Chiral 2-(o-Iodoxyphenyl)-oxazolines. Org. Lett 2009, 11, 1221; [PubMed: 19231848] (d)Ngatimin M; Gartshore CJ; Kindler JP; Naidu S; Lupton DW, The α-Halogenation of α,β-Unsaturated Carbonyls and Dihalogenation of Alkenes Using Bisacetoxyiodobenzene/Pyridine Hydrohalides. Tetrahedron Lett. 2009, 50, 6008;(e)Quideau S; Lyvinec G; Marguerit M; Bathany K; Ozanne-Beaudenon A; Buffeteau T; Cavagnat D; Chénedé A, Asymmetric Hydroxylative Phenol Dearomatization through In Situ Generation of Iodanes from Chiral Iodoarenes and *m*-CPBA. Angew. Chem. Int. Ed 2009, 48, 4605;(f)Yu J; Cui J; Hou X-S; Liu S-S; Gao W-C; Jiang S; Tian J; Zhang C, Enantioselective α-Tosyloxylation of Ketones Catalyzed by Spirobiindane Scaffold-based Chiral Iodoarenes. Tetrahedron: Asymmetry 2011, 22, 2039;(g)Kong W; Feige P; de Haro T; Nevado C, Regio- and Enantioselective Aminofluorination of Alkenes. Angew. Chem. Int. Ed 2013, 52, 2469;(h)Brenet S; Berthiol F; Einhorn J, 3,3'-Diiodo-BINOL-Fused Maleimides as Chiral Hypervalent Iodine(III) Organocatalysts. Eur. J. Org. Chem 2013, 2013, 8094;(i)Bosset C; Coffinier R; Peixoto PA; El Assal M; Miqueu K; Sotiropoulos JM; Pouységu L; Quideau S, Asymmetric Hydroxylative Phenol Dearomatization Promoted by Chiral Binaphthylic and Biphenylic Iodanes. Angew. Chem. Int. Ed 2014, 53, 9860;(j)El Assal M; Peixoto PA; Coffinier R; Garnier T; Deffieux D; Miqueu K; Sotiropoulos J-M; Pouységu L; Quideau S, Synthesis of Scyphostatin Analogues through Hypervalent Iodine-Mediated Phenol Dearomatization. J. Org. Chem 2017, 82, 11816; [PubMed: 28991470] (k)Levitre G; Dumoulin A; Retailleau P; Panossian A; Leroux FR; Masson G, Asymmetric α-Sulfonyl- and α-Phosphoryl-Oxylation of Ketones by a Chiral Hypervalent Iodine(III). J. Org. Chem 2017, 82, 11877; [PubMed: 28731345] (l)Antien K; Viault G; Pouységu L; Peixoto PA; Quideau S, Asymmetric Dearomative Spirolactonization of Naphthols Using λ3-Iodanes Under Chiral Phase-Transfer Catalysis. Tetrahedron 2017, 73, 3684;(m)Companys S; Peixoto PA; Bosset C; Chassaing S; Miqueu K; Sotiropoulos J-M; Pouységu L; Quideau S, Asymmetric Alkynylation of β-Ketoesters and Naphthols Promoted by New Chiral Biphenylic Iodanes. Chem. Eur. J 2017, 23, 13309; [PubMed: 28715080] (n)Wang Y; Yuan H; Lu H; Zheng W-H, Development of Planar Chiral Iodoarenes Based on [2.2]Paracyclophane and Their Application in Catalytic Enantioselective Fluorination of β-Ketoesters. Org. Lett 2018, 20, 2555; [PubMed: 29652155] (o)Hashimoto T; Shimazaki Y; Omatsu Y; Maruoka K, Indanol-Based Chiral Organoiodine Catalysts for Enantioselective Hydrative Dearomatization. Angew. Chem. Int. Ed 2018, 57, 7200;(p)Ding Q; He H; Cai Q, Chiral Aryliodine-Catalyzed Asymmetric Oxidative C–N Bond Formation via Desymmetrization Strategy. Org. Lett 2018, 20, 4554. [PubMed: 30036067]

(10). For selected examples on the application of chiral hypervalent iodine catalysts: Wu H; He Y-P; Xu L; Zhang D-Y; Gong L-Z, Asymmetric Organocatalytic Direct C(sp2)−H/C(sp3)−H Oxidative Cross-Coupling by Chiral Iodine Reagents. Angew. Chem. Int. Ed 2014, 53, 3466;Mizar P; Wirth T, Flexible Stereoselective Functionalizations of Ketones through Umpolung with Hypervalent Iodine Reagents. Angew. Chem. Int. Ed 2014, 53, 5993;Woerly EM; Banik SM; Jacobsen EN, Enantioselective, Catalytic Fluorolactonization Reactions with a Nucleophilic Fluoride Source. J. Am. Chem. Soc 2016, 138, 13858;Jain N; Xu S; Ciufolini MA, Asymmetric Oxidative Cycloetherification of Naphtholic Alcohols. Chem. Eur. J 2017, 23, 4542; [PubMed: 28194827] Mennie KM; Banik SM; Reichert EC; Jacobsen EN, Catalytic Diastereo-

Author Manuscript Author Manuscript Author Manuscript Author Manuscript

and Enantioselective Fluoroamination of Alkenes. J. Am. Chem. Soc 2018, 140, 4797; [PubMed: 29583001] Scheidt F; Schäfer M; Sarie J; Daniliuc C; Molloy J; Gilmour R, Enantioselective, Catalytic Vicinal Difluorination of Alkenes. Angew. Chem. Int. Ed, DOI:10.1002/anie.201810328

(11). Banik SM; Medley JW; Jacobsen EN, Catalytic, Asymmetric Difluorination of Alkenes to Generate Difluoromethylated Stereocenters. Science 2016, 353, 51. [PubMed: 27365443]

(12). (a)Hu J; Zhang W; Wang F, Selective Difluoromethylation and Monofluoromethylation Reactions. Chem. Commun 2009, 7465;(b)Rong J; Ni C; Hu J, Metal-Catalyzed Direct Difluoromethylation Reactions. Asian J. Org. Chem 2017, 6, 139;(c)Yerien DE; Barata-Vallejo S; Postigo A, Difluoromethylation Reactions of Organic Compounds. Chem. Eur. J 2017, 23, 14676. [PubMed: 28632338] (d)Feng Z; Xiao YL; Zhang X Transition-Metal (Cu, Pd, Ni)-Catalyzed Difluoroalkylation via Cross-Coupling with Difluoroalkyl Halides. Acc. Chem. Res 2018, 51, 2264. [PubMed: 30132322]

(13). Meanwell NA, Synopsis of Some Recent Tactical Application of Bioisosteres in Drug Design. J. Med. Chem 2011, 54, 2529. [PubMed: 21413808]

(14). Erickson JA; McLoughlin JI, Hydrogen Bond Donor Properties of the Difluoromethyl Group. J. Org. Chem 1995, 60, 1626.

(15). Frisch MJ; Trucks GW; Schlegel HB; Scuseria GE; Robb MA; Cheeseman JR; Scalmani G; Barone V; Mennucci B; Petersson GA; Nakatsuji H; Caricato M; Li X; Hratchian HP; Izmaylov AF; Bloino J; Zheng G; Sonnenberg JL; Hada M; Ehara M; Toyota K; Fukuda R; Hasegawa J; Ishida M; Nakajima T; Honda Y; Kitao O; Nakai H; Vreven T; Montgomery JA, Jr.; Peralta JE; Ogliaro F; Bearpark M; Heyd JJ; Brothers E; Kudin KN; Staroverov VN; Kobayashi R; Normand J; Raghavachari K; Rendell A; Burant JC; Iyengar SS; Tomasi J; Cossi M; Rega N; Millam JM; Klene M; Knox JE; Cross JB; Bakken V; Adamo C; Jaramillo J; Gomperts R; Stratmann RE; Yazyev O; Austin AJ; Cammi R; Pomelli C; Ochterski JW; Martin RL; Morokuma K; Zakrzewski VG; Voth GA; Salvador P; Dannenberg JJ; Dapprich S; Daniels AD; Farkas O; Foresman JB; Ortiz JV; Cioslowski J; Fox DJ; Gaussian 09, revision B.01; Gaussian Inc.: Wallingford, CT, 2009.

(16). Zhao Y; Truhlar DG, Density Functionals with Broad Applicability in Chemistry. Acc. Chem. Res 2008, 41, 157. [PubMed: 18186612]

(17). Hay PJ; Wadt WR, Ab Initio Effective Core Potentials for Molecular Calculations. Potentials for K to Au Including the Outermost Core Orbitals. J. Chem. Phys 1985, 82, 299.

(18). Marenich AV; Cramer CJ; Truhlar DG, Universal Solvation Model Based on Solute Electron Density and on a Continuum Model of the Solvent Defined by the Bulk Dielectric Constant and Atomic Surface Tensions. J. Phys. Chem. B 2009, 113, 6378. [PubMed: 19366259]

(19). Andrae D; Häußermann U; Dolg M; Stoll H; Preuß H, Energy-Adjusted Ab Initio Pseudopotentials for the Second and Third Row Transition Elements. Theoretica chimica acta 1990, 77, 123.

(20). (a)Sreenithya A; Sunoj RB, Mechanistic Insights on Iodine(III) Promoted Metal-Free Dual C–H Activation Involved in the Formation of a Spirocyclic Bis-oxindole. Org. Lett 2014, 16, 6224; [PubMed: 25420189] (b)Sreenithya A; Surya K; Sunoj RB, Hypercoordinate Iodine(III) Promoted Reactions and Catalysis: An Update on Current Mechanistic Understanding. WIREs Comput. Mol. Sci 2017, 7, e1299.

(21). (a)Frei R; Wodrich MD; Hari DP; Borin P-A; Chauvier C; Waser J, Fast and Highly Chemoselective Alkynylation of Thiols with Hypervalent Iodine Reagents Enabled through a Low Energy Barrier Concerted Mechanism. J. Am. Chem. Soc 2014, 136, 16563; [PubMed: 25365776] (b)Beaulieu S; Legault CY, Mechanistic Insights on the Iodine(III)-Mediated α-Oxidation of Ketones. Chem. Eur. J 2015, 21, 11206; [PubMed: 26118902] (c)Zhu C; Liang Y; Hong X; Sun H; Sun W-Y; Houk KN; Shi Z, Iodoarene-Catalyzed Stereospecific Intramolecular sp3 C–H Amination: Reaction Development and Mechanistic Insights. J. Am. Chem. Soc 2015, 137, 7564; [PubMed: 26035639] (d)Sun T-Y; Wang X; Geng H; Xie Y; Wu Y-D; Zhang X; Schaefer HF, III, Why does Togni's Reagent I Exist in the High-Energy Hypervalent Iodine Form? Re-Evaluation Of Benziodoxole Based Hypervalent Iodine Reagents. Chem. Commun 2016, 52, 5371;(e)Li M; Xue X-S; Guo J; Wang Y; Cheng J-P An Energetic Guide for Estimating Trifluoromethyl Cation Donor Abilities of Electrophilic Trifluoromethylating Reagents:

Author Manuscript Author Manuscript Author Manuscript Author Manuscript

Computations of X–CF3 Bond Heterolytic Dissociation Enthalpies. J. Org. Chem 2016, 81, 3119.; [PubMed: 26999452] (f)Jiang H; Sun T-Y; Wang X; Xie Y; Zhang X; Wu Y-D; Schaefer HF, A Twist of the Twist Mechanism, 2-Iodoxybenzoic Acid (IBX)-Mediated Oxidation of Alcohol Revisited: Theory and Experiment. Org. Lett 2017, 19, 6502. [PubMed: 29166031] (g)Li M; Wang Y; Xue X-S; Cheng J-P A Systematic Assessment of Trifluoromethyl Radical Donor Abilities of Electrophilic Trifluoromethylating Reagents Asian. J. Org. Chem 2017, 6, 235. (h)Harned AM Concerning the Mechanism of Iodine(III)-Mediated Oxidative Dearomatization of Phenols. Org Biomol Chem 2018, 16, 2324. [PubMed: 29542797]

(22). (a)Sreenithya A; Patel C; Hadad CM; Sunoj RB, Hypercoordinate Iodine Catalysts in Enantioselective Transformation: The Role of Catalyst Folding in Stereoselectivity. ACS Catal. 2017, 7, 4189;(b)Fujita M, Mechanistic Aspects of Alkene Oxidation Using Chiral Hypervalent Iodine Reagents. Tetrahedron Lett. 2017, 58, 4409;(c)Breugst M; von der Heiden D, Mechanisms in Iodine Catalysis. Chem. Eur. J 2018, 24, 9187; [PubMed: 29469220] (d)Pluta R; Krach PE; Cavallo L; Falivene L; Rueping M, Metal-Free Catalytic Asymmetric Fluorination of Keto Esters Using a Combination of Hydrogen Fluoride (HF) and Oxidant: Experiment and Computation. ACS Catal. 2018, 8, 2582.

(23). Johnson ER; Keinan S; Mori-Sánchez P; Contreras-García J; Cohen AJ; Yang W, Revealing Noncovalent Interactions. J. Am. Chem. Soc 2010, 132, 6498. [PubMed: 20394428]

(24). Lu T; Chen F, Multiwfn: A Multifunctional Wavefunction Analyzer. J. Comput. Chem 2012, 33, 580. [PubMed: 22162017]

(25). Legault CY CYLview, 1.0b; Université de Sherbrooke: (Québec) Canada, 2009; http://www.cylview.org.

(26). Humphrey W; Dalke A; Schulten K, VMD: Visual Molecular Dynamics. J. Mol. Graphics 1996, 14, 33.

(27). The ester substituent at the para-position of aryl iodide is crucial to induce high enantioselectivity for the present reaction. We have found that catalysts lacking the para-ester substituent can undergo degradation to species that are catalytically active, but poorly enantioselective. In other reactions where lower HF loadings can be usedthese degradation pathways are slower, catalysts lacking the para-ester substituent are observed to give high enantioselectivities (see ref.10c and 10e).

(28). (a)Kitamura T; Muta K; Oyamada J, Hypervalent Iodine-Mediated Fluorination of Styrene Derivatives: Stoichiometric and Catalytic Transformation to 2,2-Difluoroethylarenes. J. Org. Chem 2015, 80, 10431; [PubMed: 26450682] (b)Banik SM; Medley JW; Jacobsen EN, Catalytic, Diastereoselective 1,2-Difluorination of Alkenes. J. Am. Chem. Soc 2016, 138, 5000; [PubMed: 27046019] (c)Molnár IG; Thiehoff C; Holland MC; Gilmour R, Catalytic, Vicinal Difluorination of Olefins: Creating a Hybrid, Chiral Bioisostere of the Trifluoromethyl and Ethyl Groups. ACS Catal. 2016, 6, 7167.(d)Kitamura T; Mizuno S; Muta K; Oyamada J, Synthesis of β-Fluorovinyliodonium Salts by the Reaction of Alkynes with Hypervalent Iodine/HF Reagents. J. Org. Chem 2018, 83, 2773. [PubMed: 29431440] (e)Kitamura T; Yoshida K; Mizuno S; Miyake A; Oyamada J, Difluorination of Functionalized Aromatic Olefins Using Hypervalent Iodine/HF Reagents. J. Org. Chem 2018 DOI: 10.1021/acs.joc.8b02473

(29). For selected reviews, see: Beale TM; Chudzinski MG; Sarwar MG; Taylor MS, Halogen Bonding in Solution: Thermodynamics and Applications. Chem. Soc. Rev 2013, 42, 1667; [PubMed: 22858664] Cavallo G; Metrangolo P; Milani R; Pilati T; Priimagi A; Resnati G; Terraneo G, The Halogen Bond. Chem. Rev 2016, 116, 2478; [PubMed: 26812185] Wang H; Wang W; Jin WJ, σ-Hole Bond *vs* π-Hole Bond: A Comparison Based on Halogen Bond. Chem. Rev 2016, 116, 5072. [PubMed: 26886515]

(30). Pinto de Magalhães H; Togni A; Lüthi HP, Importance of Nonclassical σ-Hole Interactions for the Reactivity of λ^3-Iodane Complexes. J. Org. Chem 2017, 82, 11799; [PubMed: 28988483] Pinto de Magalhães H; Togni A; Lüthi HP, Importance of Nonclassical σ-Hole Interactions for the Reactivity of λ^3-Iodane Complexes. J. Org. Chem 2017, 82, 11799; [PubMed: 28988483] (c)Heinen F; Engelage E; Dreger A; Weiss R; Huber SM, Iodine(III) Derivatives as Halogen Bonding Organocatalysts. Angew. Chem. Int. Ed 2018, 57, 3830.

(31). (a)Yoneda N, Advances in the Preparation of Organofluorine Compounds Involving Iodine and/or Iodo-Compounds. J. Fluorine Chem 2004, 125, 7(b)Tao J; Tran R; Murphy GK, Dihaloiodoarenes: α,α-Dihalogenation of Phenylacetate Derivatives. J. Am. Chem. Soc 2013,

Author Manuscript Author Manuscript Author Manuscript Author Manuscript

135, 16312; [PubMed: 24152071] (c)Molnar IG; Gilmour R, Catalytic Difluorination of Olefins. J. Am. Chem. Soc 2016, 138, 5004; [PubMed: 26978593] (d)Sinclair GS; Tran R; Tao J; Hopkins WS; Murphy GK, Borosilicate Activation of (Difluoroiodo)toluene in the gem-Difluorination of Phenyldiazoacetate Derivatives. Eur. J. Org. Chem 2016, 2016, 4603;(e)Banik SM; Mennie KM; Jacobsen EN, Catalytic 1,3-Difunctionalization via Oxidative C–C Bond Activation. J. Am. Chem. Soc 2017, 139, 9152; [PubMed: 28622723] (f)Scheidt F; Thiehoff C; Yilmaz G; Meyer S; Daniliuc CG; Kehr G; Gilmour R, Fluorocyclisation via I(I)/I(III) Catalysis: a Concise Route to Fluorinated Oxazolines. Beilstein J. Org. Chem 2018, 14, 1021; [PubMed: 29977374] (g)Kohlhepp SV; Gulder T, Hypervalent Iodine(III) Fluorinations of Alkenes and Diazo Compounds: New Opportunities in Fluorination Chemistry. Chem. Soc. Rev 2016, 45, 6270. [PubMed: 27417189]

(32). Asari AH; Lam Y.-h.; Tius MA; Houk KN, Origins of the Stereoselectivity in a Thiourea–Primary Amine-Catalyzed Nazarov Cyclization. J. Am. Chem. Soc 2015, 137, 13191. [PubMed: 26426475]

(33). Nucleophilic attack of the iodine(III) center by carbonyl oxygen or the olefinic double bond of the cinnamamide have higher barriers, see Figure S4.

(34). Wirth T; Hirt UH, Chiral Hypervalent Iodine Compounds. Tetrahedron: Asymmetry 1997, 8, 23.

(35). (a)Yoneda N, The Combination of Hydrogen Fluoride with Organic Bases as Fluorination Agents. Tetrahedron 1991, 47, 5329(b)Olah GA; Welch JT; Vankar YD; Nojima M; Kerekes I; Olah JA, Synthetic Methods and Reactions. 63. Pyridinium Poly(Hydrogen Fluoride) (30% Pyridine-70% Hydrogen Fluoride): A Convenient Reagent For Organic Fluorination Reactions. J. Org. Chem 1979, 44, 3872.

(36). Zhou B; Yan T; Xue X-S; Cheng J-P, Mechanism of Silver-Mediated Geminal Difluorination of Styrenes with a Fluoroiodane Reagent: Insights into Lewis-Acid-Activation Model. Org. Lett 2016, 18, 6128. [PubMed: 27934395]

(37). It should be pointed out that the fit of the calculated overall activation free energy of 18.9 kcal mol−1 and the 60 h reaction times observed experimentally is not good. The full catalytic cycle includes iodoarene oxidation and deoxyfluorination, and either of these steps may be rate-limiting. Indeed, Kitamura and co-workers' recent study showed that, for the reaction of p-(difluoroiodo)toluene with 1-alkynes, a longer reaction time is required when using PhI than using PhIO, suggesting that iodoarene oxidation is more likely the rate-limiting step (see ref. 28d). Additioally, mass transport may also play an important role, as the actual reaction is hetereogeneous, with distinct DCM and HF-pyridine phases as well as appearance of solids.

(38). The computed activation energy difference using other methods give a similar trend, see Table S1.

(39). Wang H; Houk KN, Torsional Control of Stereoselectivities in Electrophilic Additions and Cycloadditions to Alkenes. Chem. Sci 2014, 5, 462.

(40). (a)Krenske EH; Houk KN, Aromatic Interactions as Control Elements in Stereoselective Organic Reactions. Acc. Chem. Res 2013, 46, 979 [PubMed: 22827883] (b)Wheeler SE, Understanding Substituent Effects in Noncovalent Interactions Involving Aromatic Rings. Acc. Chem. Res 2013, 46, 1029 [PubMed: 22725832] (c)Wheeler SE; Bloom JWG, Toward a More Complete Understanding of Noncovalent Interactions Involving Aromatic Rings. J. Phys. Chem. B 2014, 118, 6133(d)Wheeler SE; Seguin TJ; Guan Y; Doney AC, Noncovalent Interactions in Organocatalysis and the Prospect of Computational Catalyst Design. Acc. Chem. Res 2016, 49, 1061 [PubMed: 27110641] (e)Maji R; Mallojjala SC; Wheeler SE, Chiral Phosphoric Acid Catalysis: From Numbers to Insights. Chem. Soc. Rev 2018, 47, 1142. [PubMed: 29355873]

(41). For selected examples, see: Wheeler SE; McNeil AJ; Müller P; Swager TM; Houk KN, Probing Substituent Effects in Aryl−Aryl Interactions Using Stereoselective Diels−Alder Cycloadditions. J. Am. Chem. Soc 2010, 132, 3304 [PubMed: 20158182] Wheeler SE, Local Nature of Substituent Effects in Stacking Interactions. J. Am. Chem. Soc 2011, 133, 10262 [PubMed: 21599009] Seguin TJ; Lu T; Wheeler SE, Enantioselectivity in Catalytic Asymmetric Fischer Indolizations Hinges on the Competition of π-Stacking and CH/π Interactions. Org. Lett 2015, 17, 3066 [PubMed: 26046695] Li M; Xue X-S; Cheng J-P, Mechanism and Origins of Stereoinduction in Natural Cinchona Alkaloid Catalyzed Asymmetric Electrophilic Trifluoromethylthiolation of β-Keto Esters with N-Trifluoromethylthiophthalimide as Electrophilic SCF_3 Source. ACS Catal. 2017, 7, 7977Seguin TJ; Wheeler SE, Competing

Author Manuscript Author Manuscript Author Manuscript Author Manuscript

Noncovalent Interactions Control the Stereoselectivity of Chiral Phosphoric Acid Catalyzed Ring Openings of 3-Substituted Oxetanes. ACS Catal. 2016, 6, 7222West TH; Walden DM; Taylor JE; Brueckner AC; Johnston RC; Cheong PH-Y; Lloyd-Jones GC; Smith AD, Catalytic Enantioselective [2,3]-Rearrangements of Allylic Ammonium Ylides: A Mechanistic and Computational Study. J. Am. Chem. Soc 2017, 139, 4366 [PubMed: 28230365] Orlandi M; Coelho JAS; Hilton MJ; Toste FD; Sigman MS, Parametrization of Non-covalent Interactions for Transition State Interrogation Applied to Asymmetric Catalysis. J. Am. Chem. Soc 2017, 139, 6803 [PubMed: 28475315] Orlandi M; Hilton MJ; Yamamoto E; Toste FD; Sigman MS, Mechanistic Investigations of the Pd(0)-Catalyzed Enantioselective 1,1-Diarylation of Benzyl Acrylates. J. Am. Chem. Soc 2017, 139, 12688. [PubMed: 28800230]

(42). The ester substituent at the para-position of aryl iodide could strengthen the π···π stacking interaction. This might partially account for its crucial role to induce high enantioselectivity. However, we could not reproduce the experimental result of loss of enantioselectivity in the absence of the ester substituent at the para-position (Figure S12). In order to probe the para-substituent effect, we prepared catalysts with other electron-withdrawing para-substituents such as p-CF3 and p-CN (these results are unpublished). Those catalysts performed almost identically to the p-CO2Me substituted catalyst. This is consistent with our prediction that the para-substituent does not influence the inherent enantioselectivity of the reaction. The effects of the para ester moiety on the enantioselectivity seem much more complex than expected and worthy of further study in the future.

(43). The TS with π···π stacking interaction becomes 1.1 kcal mol^{-1} less favorable for (Z)-methyl cinnamate due to an unfavorable geometric arrangement, see Figure S11.

(44). (a)Knowles RR; Jacobsen EN, Attractive Noncovalent Interactions in Asymmetric Catalysis: Links Between Enzymes and Small Molecule Catalysts. Proc. Natl. Acad. Sci. U.S.A 2010, 107, 20678 [PubMed: 20956302] (b)Lu T; Wheeler SE, Harnessing Weak Interactions for Enantioselective Catalysis. Science 2015, 347, 719 [PubMed: 25678648] (c)Neel AJ; Hilton MJ; Sigman MS; Toste FD, Exploiting Non-Covalent π Interactions for Catalyst Design. Nature 2017, 543, 637. [PubMed: 28358089]

(45). For selected reviews of transition state stabilization by C−H···O interactions, see: Takahashi O; Kohno Y; Nishio M, Relevance of Weak Hydrogen Bonds in the Conformation of Organic Compounds and Bioconjugates: Evidence from Recent Experimental Data and High-Level ab Initio MO Calculations. Chem. Rev 2010, 110, 6049 [PubMed: 20550180] Johnston RC; Cheong PH-Y, C-H···O Non-Classical Hydrogen Bonding in the Stereomechanics of Organic Transformations: Theory and Recognition. Org. Biomol. Chem 2013, 11, 5057. [PubMed: 23824256]

(46). For selected reviews of transition state stabilization by C−H···π interactions, see: Kim KS; Tarakeshwar P; Lee JY, Molecular Clusters of π-Systems: Theoretical Studies of Structures, Spectra, and Origin of Interaction Energies. Chem. Rev 2000, 100, 4145 [PubMed: 11749343] Sobczyk L; Grabowski SJ; Krygowski TM, Interrelation between H-Bond and Pi-Electron Delocalization. Chem. Rev 2005, 105, 3513 [PubMed: 16218560] Bloom JWG; Raju RK; Wheeler SE, Physical Nature of Substituent Effects in XH/π Interactions. J. Chem. Theory Comput 2012, 8, 3167 [PubMed: 26605728] Sunoj RB, Transition State Models for Understanding the Origin of Chiral Induction in Asymmetric Catalysis. Acc. Chem. Res 2016, 49, 1019. [PubMed: 27101013]

(47). Wheeler's strategy (see ref. 41c) was employed to estimate the strength of π…π stacking interaction: see Figure S8 for details.

(48). Espinosa E; Molins E; Lecomte C, Hydrogen Bond Strengths Revealed by Topological Analyses of Experimentally Observed Electron Densities. Chem. Phys. Lett 1998, 285, 170.

Author Manuscript Author Manuscript Author Manuscript Author Manuscript

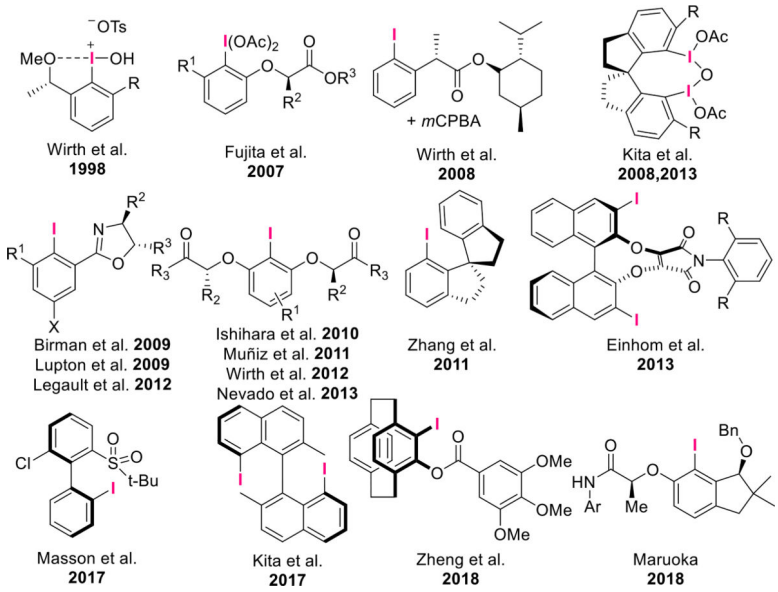

Figure 1.
Some recent chiral organoiodine reagents or catalysts.

Author Manuscript Author Manuscript Author Manuscript Author Manuscript

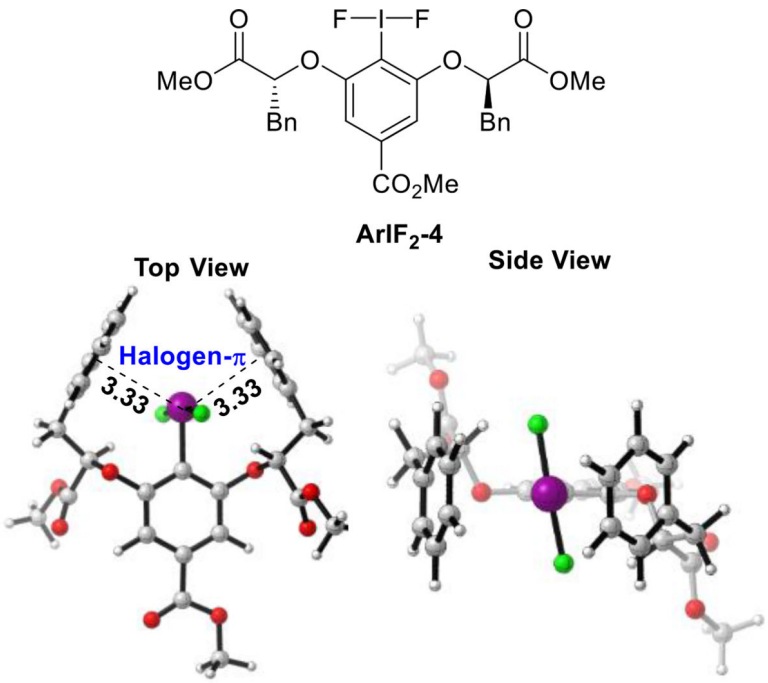

Figure 2.

The lowest-energy conformation of the active catalyst iodoarene difluoride **ArIF$_2$-4**.

Author Manuscript Author Manuscript Author Manuscript Author Manuscript

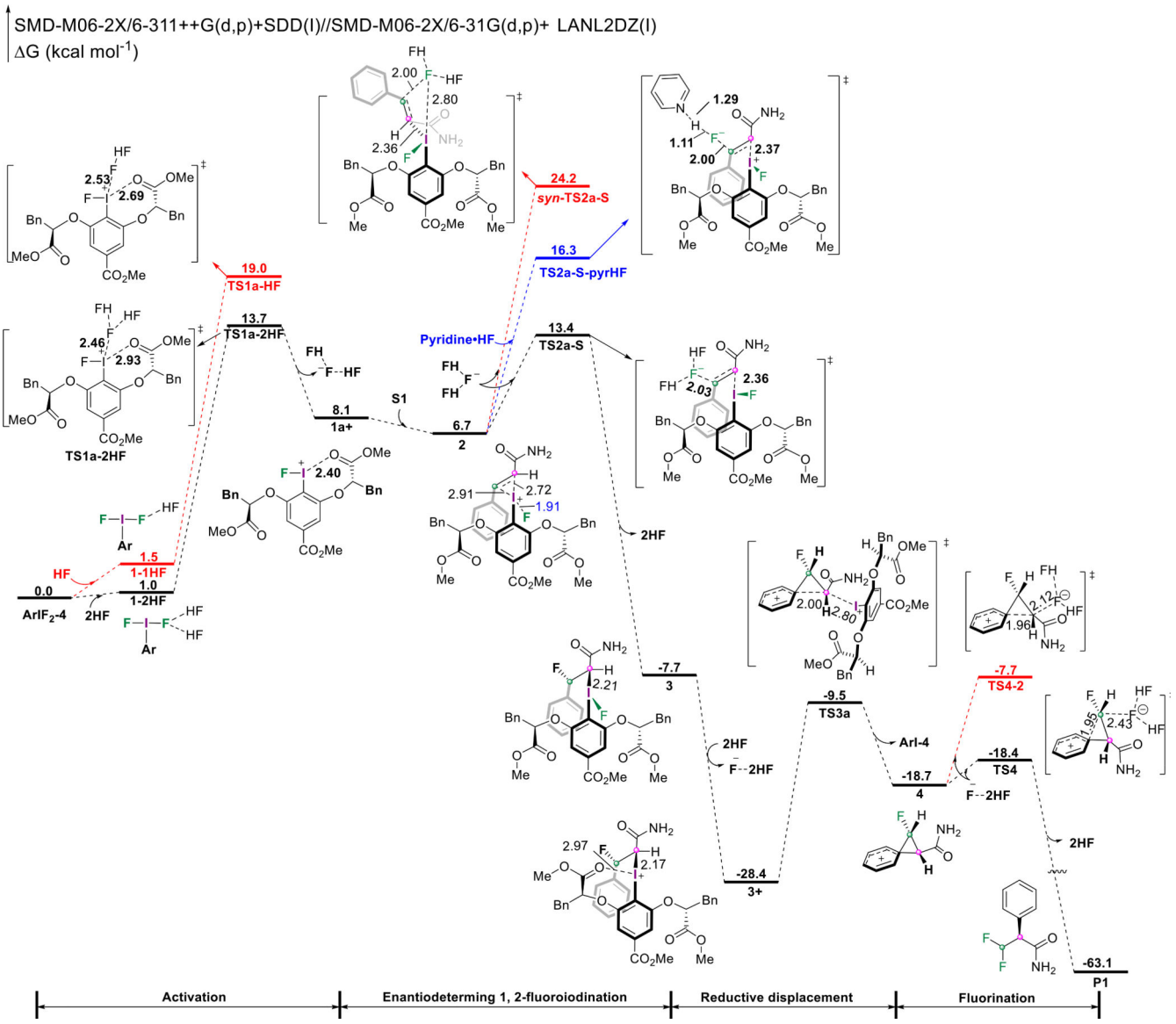

Figure 3.

Calculated potential energy profile for **ArIF$_2$-4** catalyzed asymmetric migratory geminal difluorination of cinnamamide **S1** (standard state, 1 mol L^{-1}).

Author Manuscript
Author Manuscript
Author Manuscript
Author Manuscript

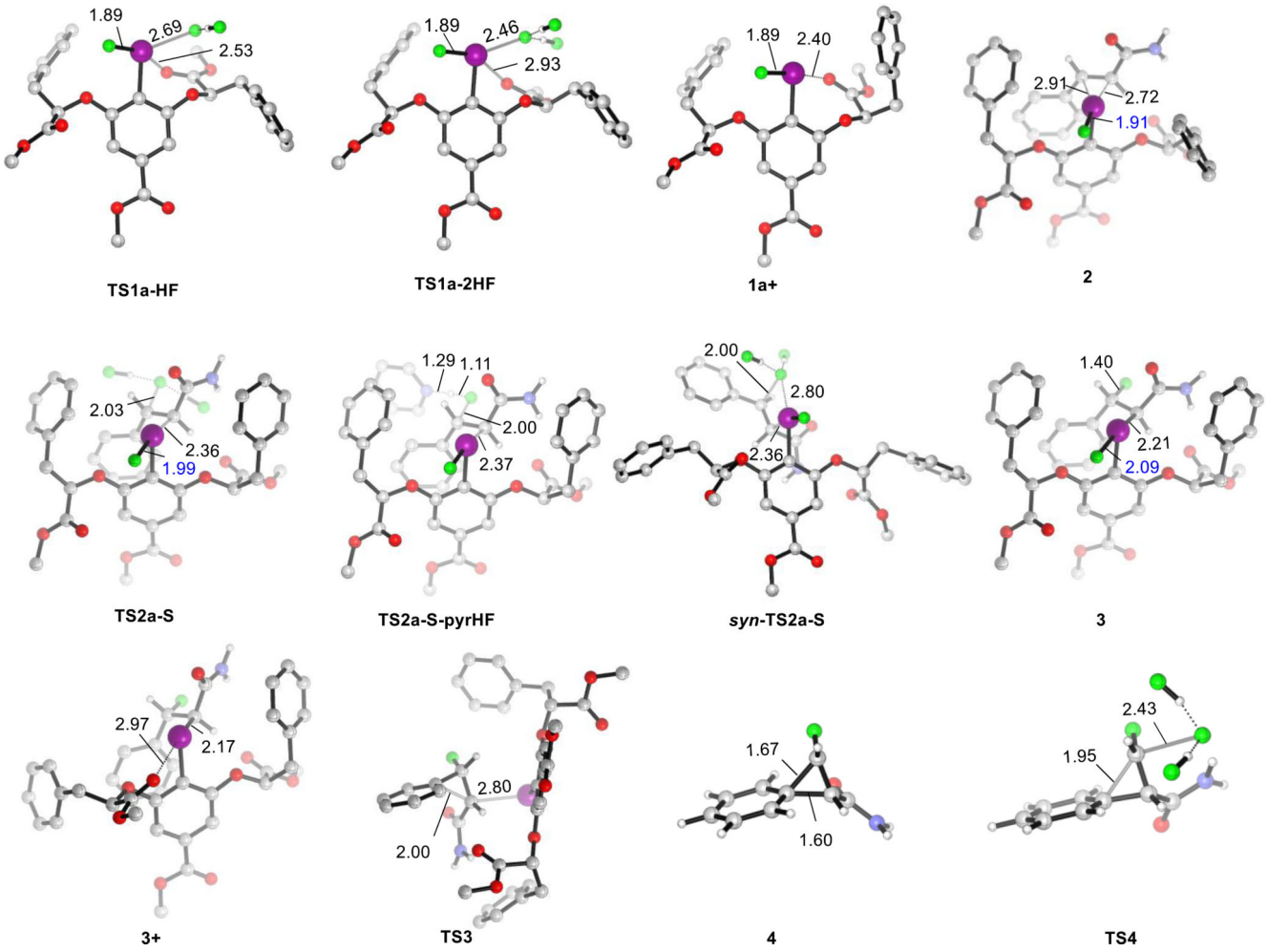

Figure 4.

Calculated geometries of transition structures and intermediates for **ArIF$_2$-4** catalyzed asymmetric migratory geminal difluorination of cinnamamide **S1**.

Author Manuscript Author Manuscript Author Manuscript Author Manuscript

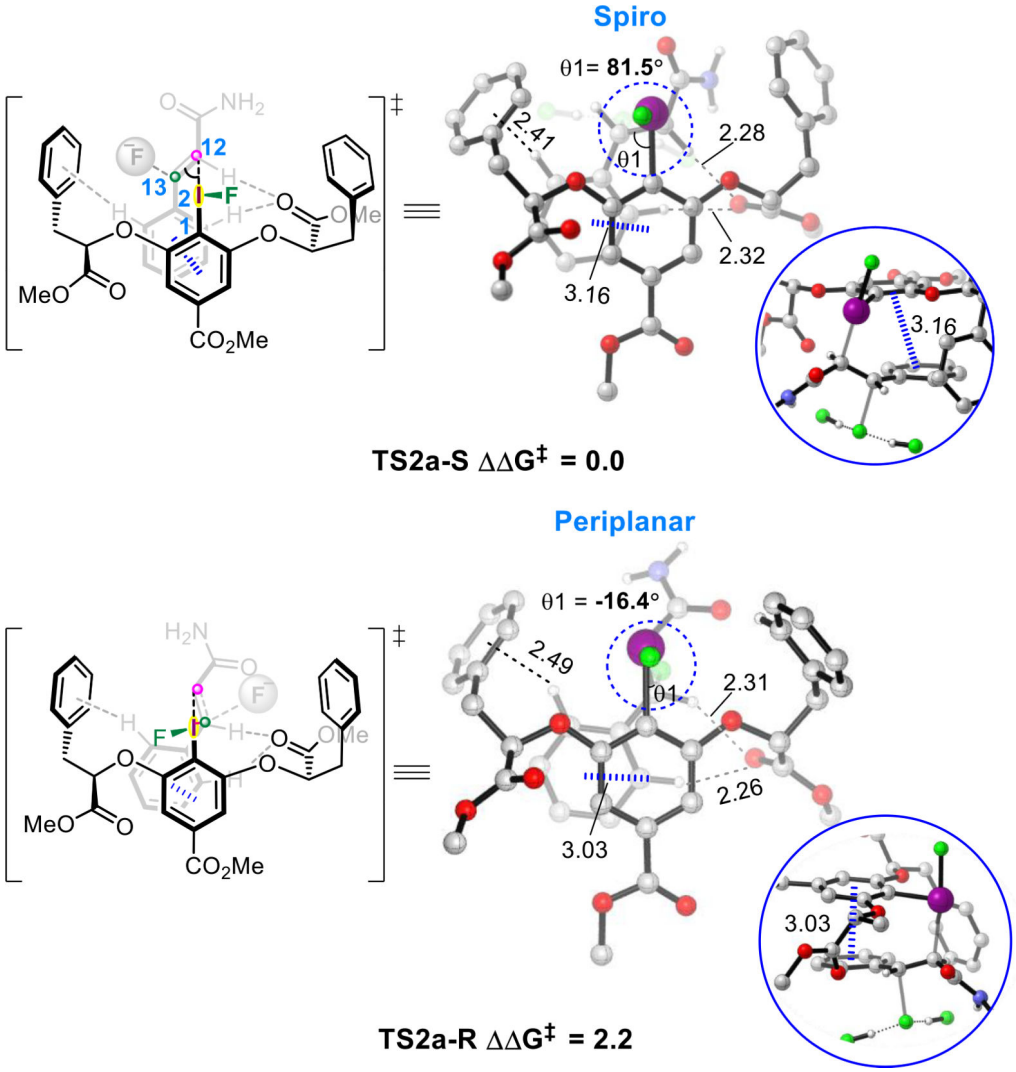

Figure 5.

Optimized enantiomeric TS geometries (some hydrogen atoms are not shown for clarity), main weak interactions, and their relative free energies (kcal mol^{-1}).

Author Manuscript Author Manuscript Author Manuscript Author Manuscript

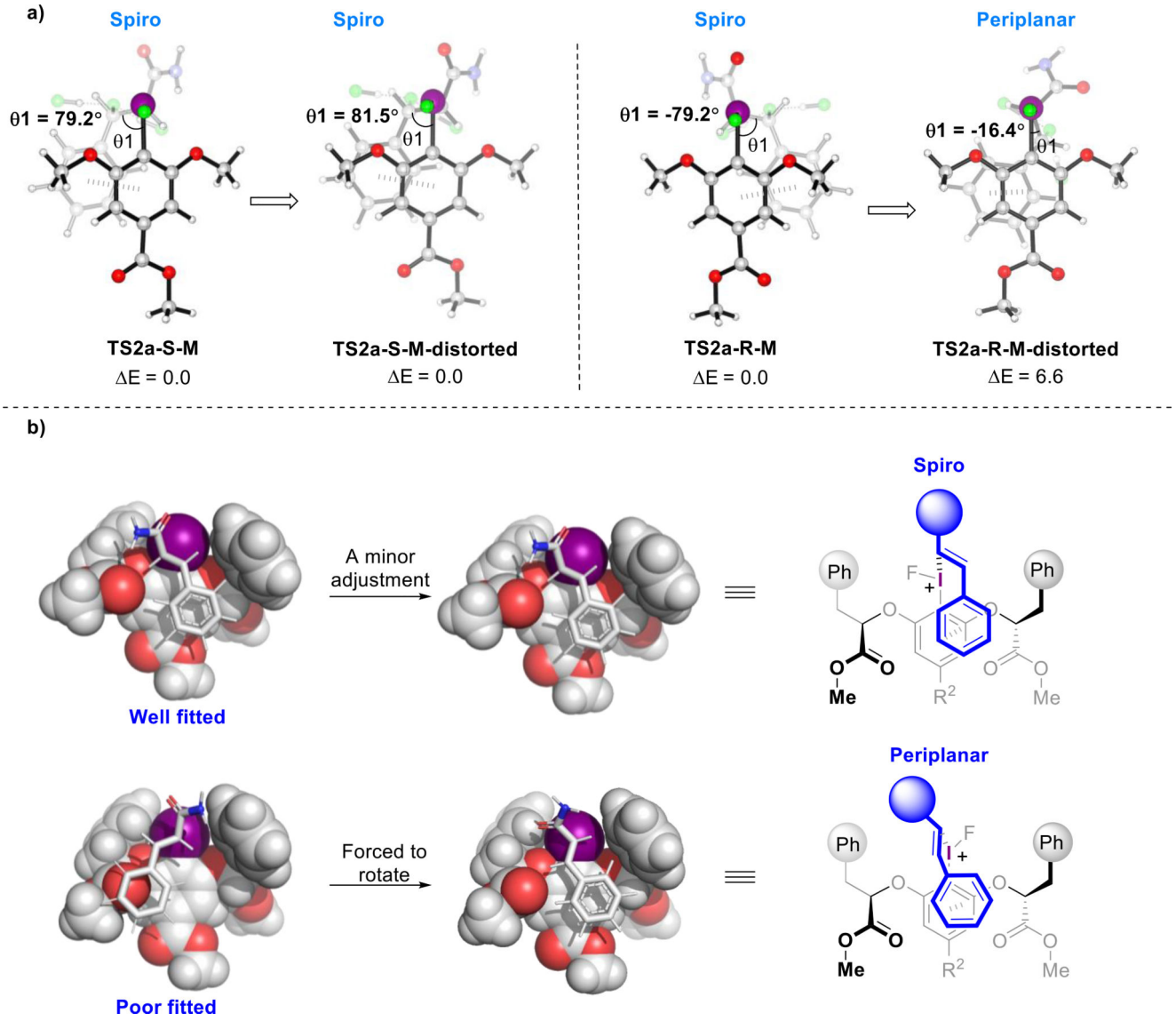

Figure 6.

a) Optimized enantiomeric TS geometries for a model catalyst and the estimated energy requires for the deviation of the ideal dihedral angle θ1 of ± 79.2°; b) Space-filling model of *Re*-face versus *Si*-face coordination of styrenes to the $I(III)^+$ center of catalyst.

Author Manuscript Author Manuscript Author Manuscript Author Manuscript

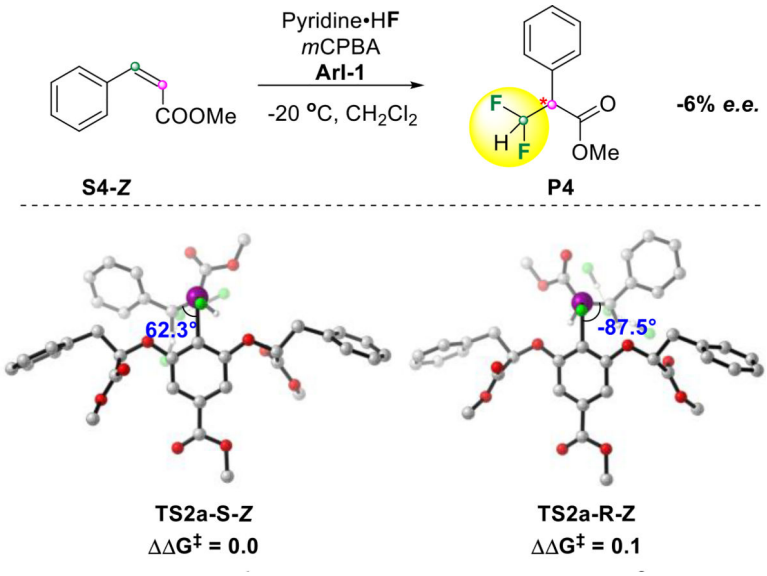

Figure 7.

Optimized enantiomeric TS geometries of asymmetric migratory geminal difluorination of (Z)-methyl cinnamate and their relative free energies (kcal mol^{-1}).

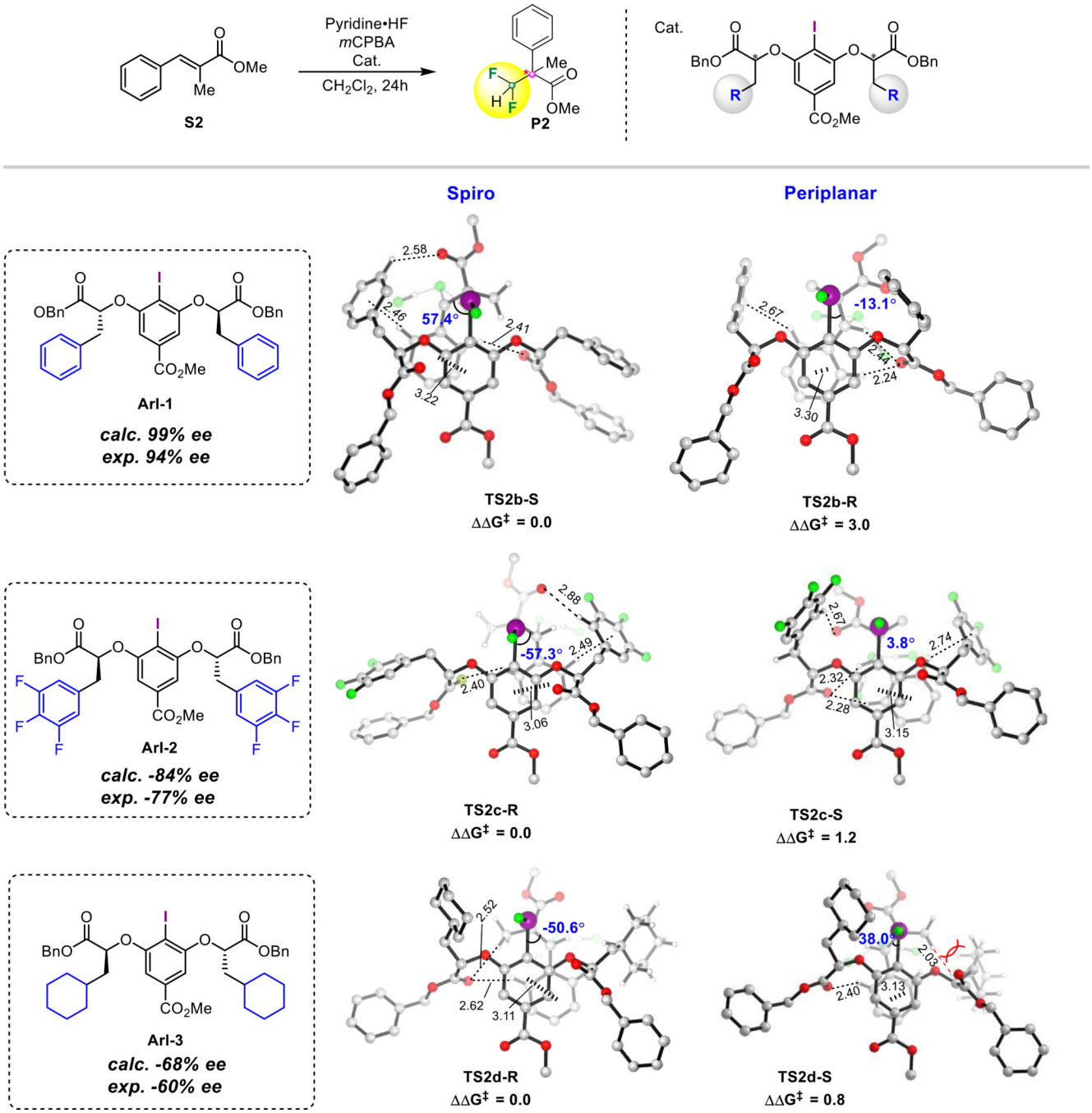

Figure 8.

Optimized stereoisomeric TS geometries and their relative free energies (kcal mol^{-1}) for precatalysts **ArI-1–3** promoted geminal difluorination of cinnamate ester **S2**.

Author Manuscript Author Manuscript Author Manuscript Author Manuscript

Author Manuscript Author Manuscript Author Manuscript Author Manuscript

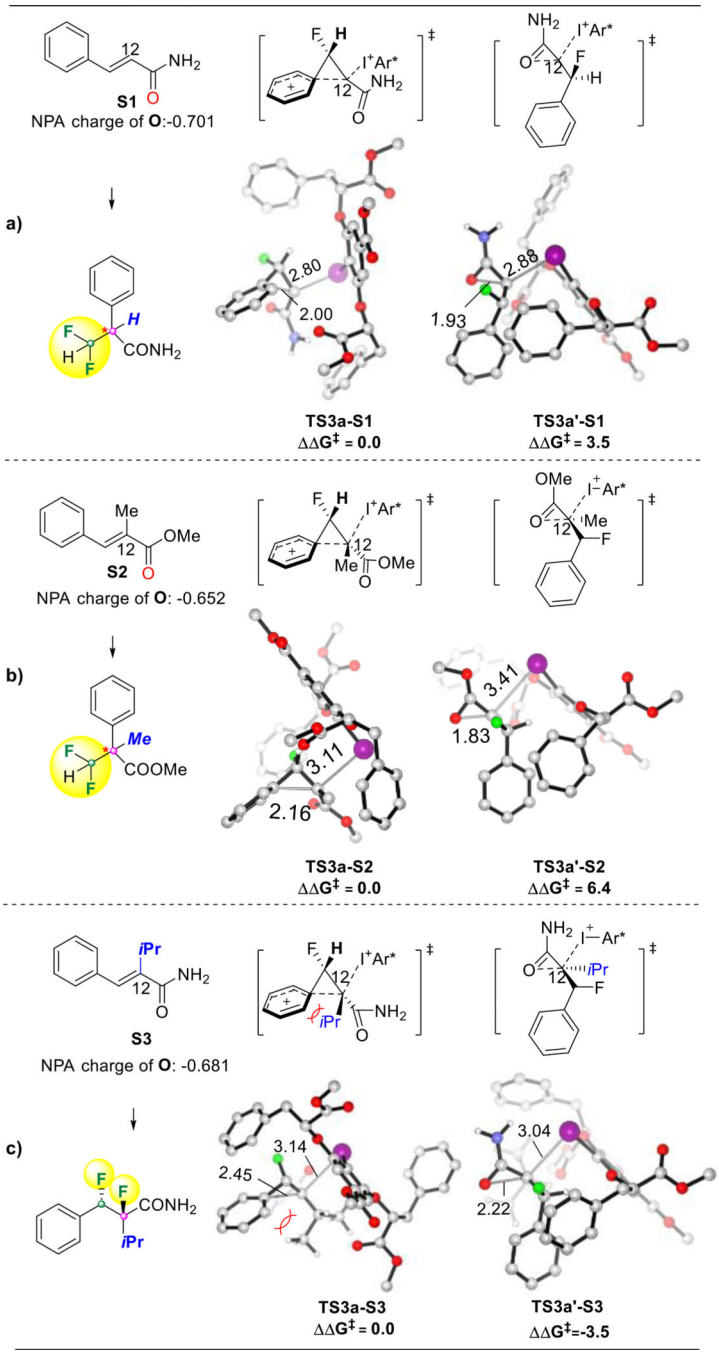

Figure 9.

Transition states for the aryl migration pathway (**TS3**) and the anchimeric assistance pathway (**TS3'**) for reactions with different substrates.

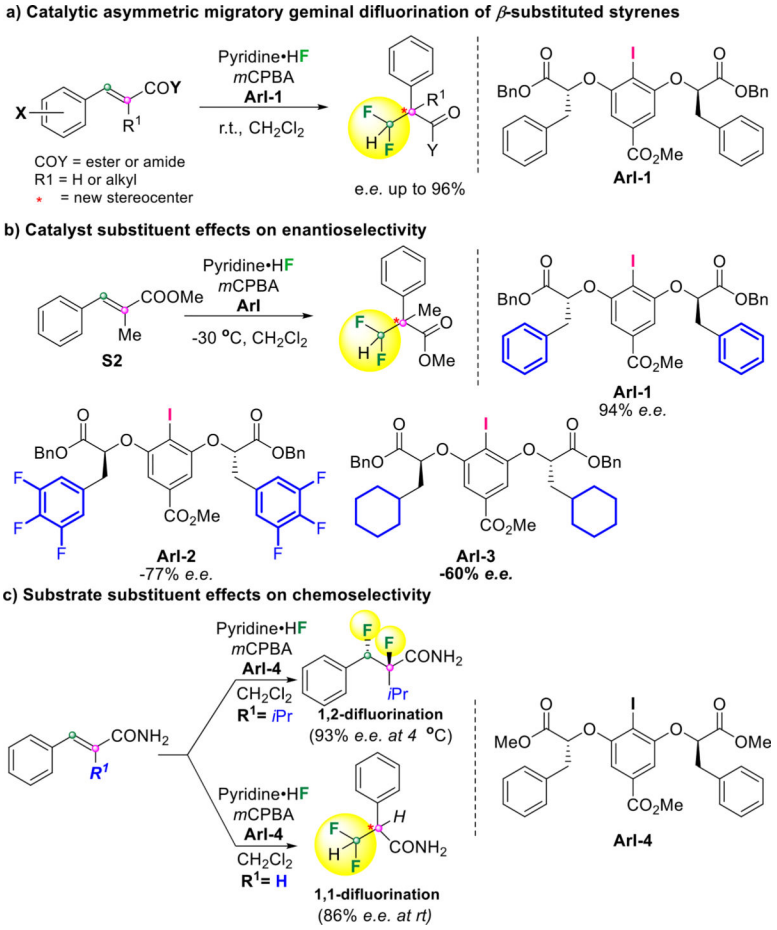

Scheme 1.

(a) Catalytic asymmetric migratory geminal difluorination of β-substituted styrenes. (b) Catalyst substituent effects on enantioselectivity. (c) Substrate substituent effects on chemoselectivity.

Author Manuscript Author Manuscript Author Manuscript Author Manuscript

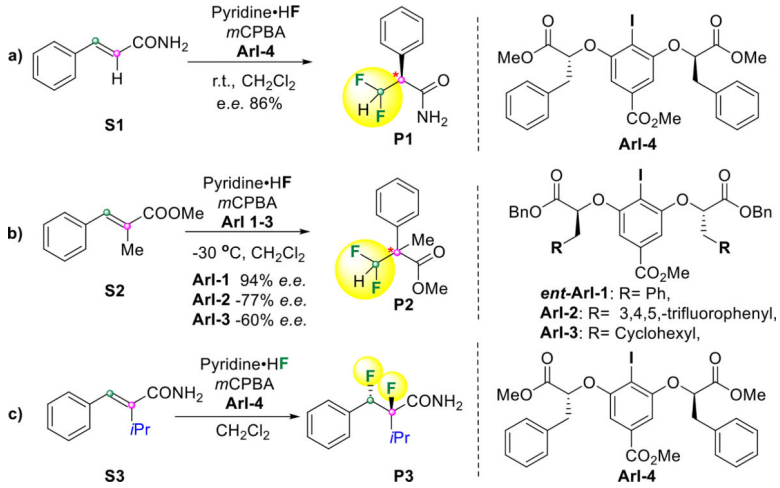

Scheme 2.
Reactions and catalysts studied computationally.

Author Manuscript Author Manuscript Author Manuscript Author Manuscript

Author Manuscript Author Manuscript Author Manuscript Author Manuscript

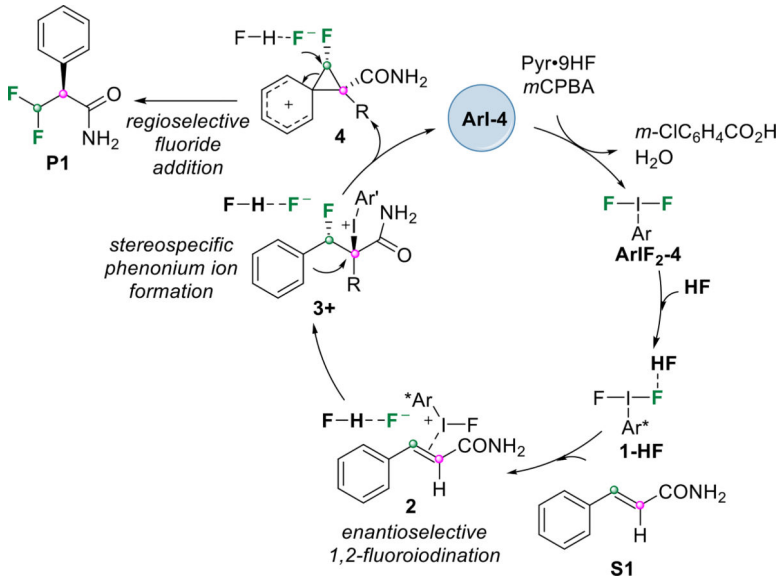

Scheme 3.

Proposed mechanism for the aryl iodide-catalyzed asymmetric migratory geminal difluorination, **S1** to **P1** in Scheme 2a.

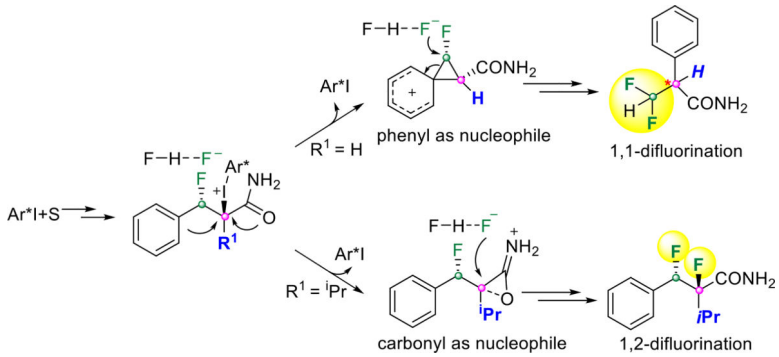

Scheme 4.

Proposed mechanism for the observed chemoselectivity.

Author Manuscript Author Manuscript Author Manuscript Author Manuscript